ELSEVIER

Earth and Planetary Science Letters 185 (2001) 135–147

EPSL

www.elsevier.com/locate/epsl

^{26}Al, ^{10}Be and U–Th isotopes in Blake Outer Ridge sediments: implications for past changes in boundary scavenging

Shangde Luo [a,*], Teh-Lung Ku [a,1], Lei Wang [a,2], John R. Southon [b], Steve P. Lund [a], Martha Schwartz [a]

[a] *Department of Earth Sciences, University of Southern California, Los Angeles, CA 90089-0740, USA*
[b] *Center for Accelerator Mass Spectrometry, Lawrence Livermore National Laboratory, Livermore, CA 94550, USA*

Received 20 March 2000; accepted 4 December 2000

Abstract

We have investigated the distributions of ^{26}Al, ^{10}Be, U–Th isotopes, and stable ^{27}Al and ^{9}Be in core CH88-11P (30°40′N, 74°41′W; 3337 m) from the Blake Outer Ridge (BOR) in the western North Atlantic, an area that is characterized by high terrigenous input. Results show authigenic ^{26}Al/^{27}Al of $< 2–8 \times 10^{-14}$ (atom/atom), authigenic ^{10}Be/^{9}Be of $0.5–2.6 \times 10^{-8}$ (atom/atom), $< 0.2–1.8 \times 10^{6}$ atoms/g of ^{26}Al, and $5.3–15.1 \times 10^{8}$ atoms/g of ^{10}Be in the core over the last glacial/interglacial cycle. These values, as well as total $^{230}Th_{ex}/^{232}Th$ and ^{10}Be/^{9}Be ratios, were all at their minima during the last glacial maximum (LGM), reflecting intensified terrestrial influx to the area. Aluminosilicate material (clays) in this influx preferentially scavenged ^{230}Th over the two other particle-reactive nuclides, ^{26}Al and ^{10}Be, such that their boundary scavenging during LGM followed the order $^{230}Th > {}^{10}Be > {}^{26}Al$, as opposed to $^{10}Be \geq {}^{230}Th > {}^{26}Al$ in the Holocene. They appear at variance with the order $^{10}Be > {}^{26}Al \approx {}^{230}Th$ as would be predicted from the relative particle reactivities of the three species. These scavenging characteristics point to ^{10}Be/^{26}Al as a potentially more suitable proxy for paleoproductivity than $^{10}Be/^{230}Th_{ex}$. Mass-balance considerations for ^{26}Al and ^{10}Be show a five-fold LGM-to-Holocene increase in deep-water circulation in the study area, with little change in ocean productivity except during the deglaciation when it increased noticeably.

Keywords: Blake-Bahama Outer Ridge; Be-10; Al-26; Th-230; productivity; paleo-oceanography

1. Introduction

In the marine environment, the isotope pairs ^{26}Al–^{27}Al, ^{10}Be–^{9}Be and ^{230}Th–^{232}Th each consists of a component (^{26}Al, ^{10}Be, ^{230}Th) with dominantly authigenic source and pathway, and a component (^{27}Al, ^{9}Be, ^{232}Th) that owes its origin essentially to detrital input from continents. In addition, the three elements Al, Be, and Th

* Corresponding author. E-mail: sluo@usc.edu

[1] Also corresponding author. E-mail: rku@usc.edu
[2] Present address: EMS Laboratories, Pasadena, CA 91105, USA.

0012-821X/01/$ – see front matter
PII: S0012-821X(00)00372-1

show different particle reactivities, hence different scavenging times, in the ocean. Because of these characteristics, the distributions of their isotopes in marine sediments contain information on past variations in particle flux, ocean mixing, and productivity ([1,2] and references therein). With these considerations in mind, we report here an investigation of the downcore distribution of isotopes of Al (^{26}Al, ^{27}Al), Be (^{10}Be, ^{9}Be), U (^{238}U, ^{234}U), and Th (^{232}Th, ^{230}Th) in a sediment core from a deep-water ocean-margin area of the Atlantic.

Cosmogenic ^{26}Al (half-life 0.72 Myr) and ^{10}Be (half-life 1.5 Myr) enter the ocean primarily through wet/dry precipitation and deposited to the seafloor by particle scavenging. Advances in accelerator mass spectrometry (AMS) have facilitated their use as geochemical and geophysical tracers in the ocean. However, the tracer utility of ^{26}Al has been less explored than that of ^{10}Be owing to the low production rate of ^{26}Al in the atmosphere and the high abundance of ^{27}Al in the crust [3–5]. The few AMS ^{26}Al analyses thus far performed on marine deposits were mostly from the Pacific Ocean where the deposition rate of terrigenous ^{27}Al is low [5–8]. The seawater concentration of ^{26}Al has only recently been found to be of the order of 10^2 atoms/kg [1].

^{26}Al in deep-sea sediments resides mainly in the authigenic (hydrogenous) phase [2]. An NaOH-leach technique has been developed [2] to quantitatively extract ^{26}Al from sediments with minimal contamination of the detrital ^{27}Al. Using this technique, we measured ^{26}Al and ^{10}Be in CH88-11P, a piston core retrieved from the Black Outer Ridge (BOR). This first data set on ^{26}Al from the Atlantic Ocean provides new insights into the geochemical behavior and tracer utility of ^{26}Al in an ocean-margin area with high terrestrial (hence ^{27}Al) input. Along with data on uranium-series isotopes, it permits us to assess past changes in terrigenous particle flux and ocean productivity at BOR, and its water exchange with the open Atlantic.

2. Sampling location and methods

The 17-m core CH88-11P was collected in 1988 aboard R/V *Cape Hatteras* from the Blake Outer Ridge (30°40′N and 74°41′W, 3337 m) [9]. The site represents a 700 km long contourite drift deposit on the continental rise off SE U.S. (Fig. 1). Coring was done on a topographic high along the crest of the ridge minimally influenced by turbidites or debris-flows which are further barred from entering the area by the vigorous northerly transport of the Gulf Stream along the western margin of the Blake Plateau. Formation of the BOR drifts is primarily caused by the southward transport of abyssal sediments entraining the western boundary undercurrent (WBUC) [9].

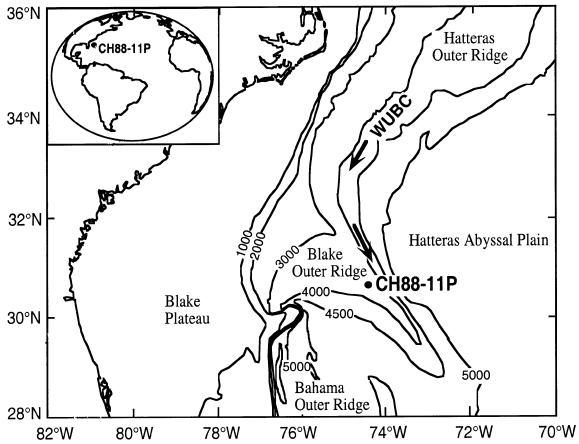

Fig. 1. Map of study area showing the location of CH88-11P (30°40′N, 74°41′W; 3337 m). The main axis of the western boundary undercurrent (WBUC) is indicated by arrows at ~4000 m isobath. CH88-11P accumulated ~4 cm/kyr in the Holocene and ~50 cm/kyr during LGM [14]. It has ~40% carbonate near the core top, which decreases to <10% in the LGM section [9]. Biogenic silica decreases from ~4% in Holocene to <1% in the LGM sediments.

Selected 5-cm intervals were analyzed for authigenic Al (^{26}Al and ^{27}Al) and Be (^{10}Be and ^{9}Be) using the NaOH-leaching technique [2]. Analyses were made by AMS (^{26}Al and ^{10}Be), atomic absorption spectrophotometry (^{27}Al) and electron-capture gas chromatography (^{9}Be) [13,14]. For the ^{26}Al analysis, ^{27}Al present in the NaOH leachate was used as carrier for ^{26}Al. During the first batch of experiments involving eight samples, the <1 mg ^{27}Al recovered from 1 g sized samples gave too weak a current for the AMS ^{26}Al anal-

Table 1
^{10}Be and ^{26}Al[a] in core CH88-11P and model estimates of water replacement rate constant (k_w), water-column residence time of ^{10}Be (τ_{Be}), and material fluxes to the BOR seafloor over the past 100 ka

Depth (cm)	Age[b] (ka)	^{10}Be (10^8 at/g)	f^c_{Be10}	f^c_{Be9}	^{26}Al (10^6 at/g)	f^c_{Al27}	k_w (10^{-2} yr^{-1})	τ_{Be} (yr)	F_p (mg/cm^2/yr)	F_p* (mg/cm^2/yr)	(F_p*−F_p) (mg/cm^2/yr)
7.5	1.5	10.5±0.2	0.81	0.35	0.6±0.2	0.018	4.4±1.8	18±6	3.7±1.3	40±14	36±14
27.5	5.4	11.8±0.2	0.81	0.42	nm						
87.5	11.9	6.2±0.1	0.48	0.24	<0.2	0.006	>2.3	<5	>18.1	>138	>120
107.5	12.5	8.0±0.1	0.54	0.23	<0.2	0.006	>4.0	<6	>16.9	>119	>102
127.5	13.1	6.4±0.1	0.37	0.13	nm						
279.0	16.9	5.7±0.1	0.31	0.17	nm						
339.0	18.5	5.3±0.1	0.19	0.10	<0.4	0.008	>0.8	<8	>29.2	>88	>59
439.0	21.0	6.9±0.1	0.35	0.14	nm						
499.0	22.5	8.9±0.1	0.57	0.22	0.8±0.3	0.016	1.0±0.7	21±9	5.1±2.2	35±14	30±14
722.0	33.5	11.0±0.1	0.69	0.38	nm						
842.0	42.8	10.9±0.1	0.70	0.40	nm						
961.0	51.7	8.9±0.1	0.69	0.42	nm						
1342.0	67.1	8.5±0.1	0.56	0.22	nm						
1542.0	78.4	13.7±0.2	0.83	0.46	1.6±0.4	0.024	1.5±0.6	35±8	1.5±0.3	21±5	19±5
1622.0	86.2	15.1±0.2	0.83	0.49	1.8±0.2	0.026	1.1±0.3	21±3	2.3±0.3	34±5	32±5
1702.0	99.0	15.1±0.2	0.83	0.48	1.7±0.5	0.021	1.5±0.7	29±9	1.7±0.5	25±7	23±7

F_p: terrigenous, F_p*: terrigenous+biogenic, and (F_p*−F_p): biogenic.
[a]Detailed data are available from the **EPSL Online Background Dataset**. nm, not measured. Upper-bound ^{26}Al values are based on detection-limit estimates. The quoted errors for ^{26}Al and ^{10}Be are one standard deviation derived from counting statistics; those for the model parameters were estimated through error propagation.
[b]The chronology is based on correlating the records of δ^{18}O, carbonate, and paleomagnetism in the core [9,10] with those in other AMS-^{14}C dated North Atlantic cores [11,12].
[c]f_{Be10} and f_{Be9} are fractions of authigenic ^{10}Be and ^{9}Be calculated from the Be data (Fig. 1a) via Eqs. 1 and 2, respectively; f_{Al27} is the fraction of authigenic Al determined by NaOH leaching.

yses. Therefore, only the ^{10}Be results are reported for these eight samples.

Al and Be were purified by cation exchange (Bio-Rad, AG 50 W×12, 200–400 mesh, 0.5 M HCl conditioned [14]). Be was eluted off with 7 cv (column volume) of 1 M HCl, and Al, with 3 cv of 4 M HCl. They were separately precipitated as $Be(OH)_2$ and $Al(OH)_3$, converted to BeO and Al_2O_3 in a Pt crucible by burning over a Bunsen burner for ~1 h, and then admixed with Ag powder in a 1:3 proportion for AMS analyses.

Totally dissolved ~1-g samples were also analyzed for ^{27}Al, ^{10}Be, and ^{9}Be, in addition to isotopes of U (^{238}U and ^{234}U) and Th (^{232}Th and ^{230}Th) [14]. ^{26}Al was not measured because of too low ^{26}Al/^{27}Al ratios. In these samples, further separation of Be from Ti after ion exchange was needed by dissolving the $Be(OH)_2$ precipitate with 3 M NaOH, removing the insoluble $Ti(OH)_4$ by centrifugation, and re-precipitating $Be(OH)_2$ from the supernatant by neutralizing with HCl.

3. Results and discussion

For detailed measurement data on Al, Be and/or U–Th isotopes, see Tables A1–A3 in the **EPSL Online Background Dataset**[3].

3.1. Influence of terrestrial particle flux on ^{10}Be/^{9}Be in sediments

^{10}Be and ^{9}Be in both the NaOH leachates and total sediments in CH88-11P are shown in Table 1 and Fig. 2a. The leached ratio of 2.6×10^{-8} in surface sediment, which reflects the dissolved ^{10}Be/^{9}Be in Holocene deep water [2], agrees well with 2.4×10^{-8} measured at a nearby ocean-margin site by Bourles et al. [15] using a leaching technique involving 1 M $MgCl_2$, 1 M NaOAc at

[3] http://www.elsevier.nl/locate/epsl; mirror site: http://www.elsevier.com/locate/epsl

pH ~5, but lower than $\sim 4\times10^{-8}$ [16] for seawater at similar depths in the open N. Atlantic (e.g. Sargasso Sea). The lower ratio at BOR probably reflects the relatively high lithogenic particle flux at ocean margins.

Deep-water $^{10}Be/^{9}Be$ of 0.5×10^{-8} in LGM is about one fifth the Holocene ratio. The low LGM value, also seen in the total $^{10}Be/^{9}Be$ (Fig. 2a), can be chiefly ascribed to an increase of continental ^{9}Be flux to the core site during glacial times. Data on Th and Al, to be shown later, support this possibility. Another possibility could be an LGM reduction of water exchange between BOR and the open Atlantic, as the reduction would decrease the boundary scavenging of ^{10}Be, hence the authigenic $^{10}Be/^{9}Be$ ratio in glacial sediments.

While particle scavenging may decrease seawater concentrations of both ^{10}Be and ^{9}Be, the ^{9}Be decrease is countered by a release of ^{9}Be from lithogenic particles. This counter effect is negligible for ^{10}Be as the dissolved ^{10}Be is mostly of atmospheric origin. Thus a high lithogenic influx during LGM tended to lower the seawater concentration of ^{10}Be but not that of ^{9}Be. The high LGM lithogenic flux also had the effect of lowering the fraction of authigenic ^{10}Be (f_{Be10}) in sediments, which can be estimated as:

$$f_{Be10} = 1-\frac{(C_{Be10}/C_{Be9})_d}{(C_{Be10}/C_{Be9})_t} \quad (1)$$

where C is concentration, with subscripts d and t denoting detrital and total sediments, respectively. The detrital $^{10}Be/^{9}Be$ at BOR can be taken as $(0.22\pm0.03)\times10^{-8}$ because (1) detrital sediments from an adjacent station DSDP68–502 (11°30′N, 79°23′W, 3051 m) has a ratio of $(0.21\pm0.02)\times10^{-8}$ [15], and (2) a riverine particulate $^{10}Be/^{9}Be$ ratio of $(0.23\pm0.03)\times10^{-8}$ is estimated from the average ^{10}Be concentration of $(4.42\pm0.55)\times10^{8}$ atoms/g (corrected for lower ^{10}Be retentivity in sand) in modern river sediments along a transect from the Atchafalaya River to the Gulf of Mexico [17], assuming 2.8 ppm of ^{9}Be in riverine particles [18]. We estimate from Eq. 1 that f_{Be10} varies from ~0.2 during the LGM to ~0.8 during interglacial periods (Table 1). Knowing f_{Be10}, we also calculate the fraction of authigenic ^{9}Be by:

$$f_{Be9} = \frac{(C_{Be10}/C_{Be9})_t}{(C_{Be10}/C_{Be9})_a} f_{Be10} \quad (2)$$

where subscript a stands for authigenic. f_{Be9} was ~0.1 during LGM and ~0.4 during interglacial times (Table 1). Thus both ^{10}Be and ^{9}Be in LGM sediments at BOR are mostly of detrital origin as a result of intensified continental flux.

3.2. $^{26}Al/^{27}Al$ in sediments and tracing authigenic deposition of ^{27}Al

The low authigenic Al of 1–2% in CH88-11P (Table 1), as opposed to ~17% in Pacific pelagic sediments [14], has contributed to the relatively large measurement errors of $^{26}Al/^{27}Al$. Fig. 2b shows an authigenic $^{26}Al/^{27}Al$ of $(3\pm1)\times10^{-14}$ in surface layers, which is about 4–6 times lower than that of $(11–19)\times10^{-14}$ in equatorial Pacific surface sediments [14]. For some LGM sediments, only the upper-limit values can be assigned. Taking these ratios as modern deep-water $^{26}Al/^{27}Al$, and mean ^{27}Al concentrations of 20 nM in deep N. Atlantic [19] and 2 nM in deep equatorial Pacific [20], we estimate deep-water ^{26}Al concentrations of 360 ± 120 atoms/l in the N. Atlantic and 130–230 atoms/l in the equatorial Pacific. These estimates are in the same order as the measured 20–200 atoms/l for the upper 1000 m of the central equatorial Pacific [1]. Thus in spite of the one-order difference in ^{27}Al concentration between the two oceans at depth, the ^{26}Al concentrations are comparable, indicating that residence times of ^{26}Al at BOR and in the equatorial Pacific are similar. Using a $^{26}Al/^{10}Be$ of $(3.8\pm0.6)\times10^{-3}$ in stratospheric air filter [21] and a global mean ^{10}Be flux of 1.2×10^{6} atoms/cm^2/yr [22], we estimate an atmospheric ^{26}Al flux of $(4.6\pm0.7)\times10^{3}$ atoms/cm^2/yr. This flux and the ^{26}Al concentration of 360 ± 120 atoms/l in BOR deep water give a residence time of ~26 yr for ^{26}Al, similar to that of ^{230}Th [23] but at least one order smaller than that of ^{10}Be in the open N. Atlantic [16].

The above discussion serves to sharpen the difference between Al and Be in their marine isotope

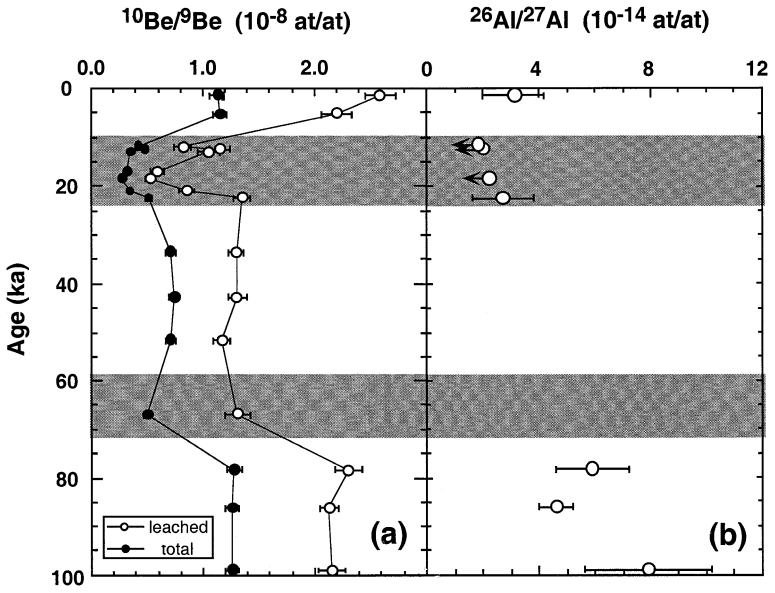

Fig. 2. (a) NaOH-leached and total $^{10}Be/^{9}Be$ and (b) NaOH-leached $^{26}Al/^{27}Al$ in CH88-11P. The arrows in (b) indicate the upper-bound $^{26}Al/^{27}Al$ values as dictated by the detection limits. Shaded areas delineate marine isotope stages 2 and 4.

geochemistries. In response to changes of terrigenous particle flux and ocean circulation, oceanic concentrations of ^{27}Al are subject to greater variations than those of ^{26}Al. In contrast, ^{9}Be in the deep ocean shows a much more uniform distribution than ^{10}Be. This difference in behavior between Al and Be reflects that whereas the fallouts of cosmogenic ^{10}Be and ^{26}Al are more or less uniform over the world ocean, rock-derived ^{9}Be and ^{27}Al are preferentially delivered to the Atlantic, and that the scavenging time of Al is much shorter than that of Be. For Be, its scavenging time is comparable to the ocean mixing time [16]. The pacificward enrichment of ^{10}Be can be attributed to the 'nutrient' effect of accumulation of ^{10}Be in deep waters due to particle remineralization, while the near uniformity in ^{9}Be could result from a chance balance between the input and the nutrient effect [24]. For the more reactive Al, the distributions of both ^{26}Al and ^{27}Al reflect their input patterns.

One would expect that ^{26}Al is subject to much less intense boundary scavenging than ^{10}Be, and this we will show later to be the case at BOR. In fact, ^{26}Al shows even less intense boundary scavenging than ^{230}Th, providing a more reliable tracer for flux of particles or particle-bound chemical species in the ocean. The tracer utility of ^{26}Al is also fostered by the constancy of ^{26}Al flux observed in equatorial Pacific sediments [14]. While an increased ^{27}Al flux occurs in the productive equatorial Pacific [25], there is no correspondence of an enhanced scavenging of ^{26}Al [14]. The oceanic distribution and scavenging of ^{26}Al and ^{27}Al may differ on account of their source–function differences.

Authigenic $^{26}Al/^{27}Al$ in CH88-11P shows a range of < 1.8–7.9×10^{-14} during the last 100 kyr, with low values in the LGM interval reflecting the high continental particle input (Fig. 2b). As the atmospheric influx of ^{26}Al is rather uniform, this ratio should be inversely related to terrigenous particle flux and serve to constrain the authigenic ^{27}Al flux. For example, given a core top authigenic $^{26}Al/^{27}Al$ of $(3.1 \pm 1.1) \times 10^{-14}$ and an atmospheric ^{26}Al flux of $(4.6 \pm 0.7) \times 10^{3}$ atoms/cm^2/yr, the present-day authigenic ^{27}Al flux at BOR should be $(1.5 \pm 0.6) \times 10^{17}$ atoms/cm^2/yr or 6.6 ± 2.6 μg/cm^2/yr. For $f_{Al} \approx 0.02$ (Table 1) and an Al content of 8% in continental rocks

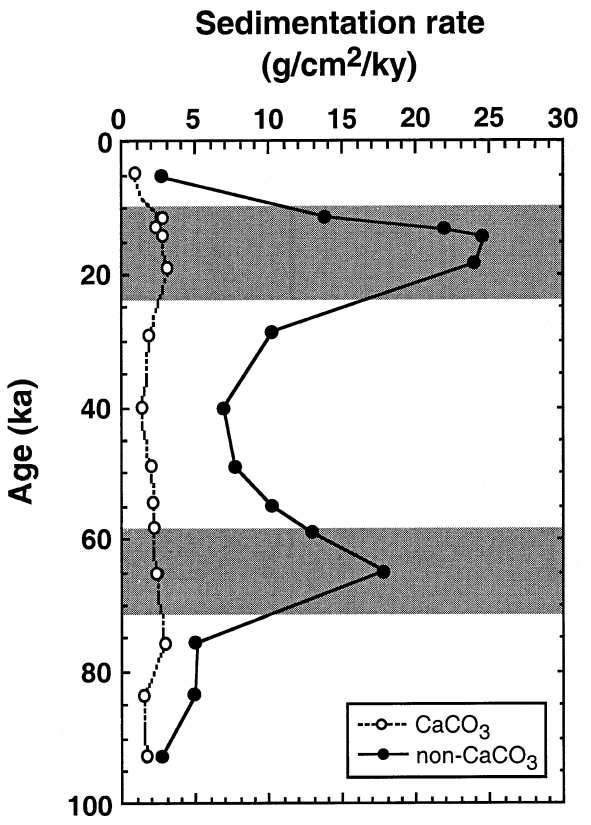

Fig. 3. Variations in carbonate and non-carbonate (terrigenous) sedimentation rates in CH88-11P, estimated based on $\delta^{18}O$ stratigraphy [9,10]. Shaded areas delineate marine isotope stages 2 and 4.

[18], the authigenic ^{27}Al flux is translated into a lithogenic particle flux of 4.1 ± 1.6 g/cm^2/kyr for the Holocene, which agrees well with the $\delta^{18}O$ stratigraphy-based estimate (Fig. 3).

3.3. $^{230}Th_{ex}/^{232}Th$ as indicator of terrestrial particle flux

Shown in Fig. 4 is the distribution of Th isotopes, in which data on $^{230}Th_{ex}$ are of particular interest because $^{230}Th_{ex}$ has often been used to normalize water-column deposition rates of chemical species such as ^{10}Be [26–32]. Neglecting any ^{238}U–^{234}U disequilibrium and assuming a detrital $^{230}Th/^{232}Th$ ratio of 0.6 ± 0.04 in BOR sediments [27], the decay-corrected activities of authigenic ^{230}Th can be estimated as:

$$^{230}Th_{ex} = (^{230}Th_m - 0.6 \times ^{232}Th_m)e^{\lambda t} - ^{238}U_a \times (e^{\lambda t} - 1) \quad (3)$$

where subscripts m and a denote measured and authigenic activities, respectively, λ is the decay constant of ^{230}Th, and t is the sediment age. As the total $^{238}U/^{232}Th$ of ~ 0.6 in BOR sediments approximates those in marine aluminosilicate detritus [33,34], U in BOR sediments is essentially detrital in origin, a fact also indicated by the measured $^{234}U/^{238}U$ being mostly close to unity.

The $^{230}Th_{ex}$ activities mirror those of ^{232}Th and were three- to four-fold lower during oxygen isotope stages 2 and 4 than during interglacial times (Fig. 4). As ^{230}Th is precipitated from water-column at a constant rate whereas ^{232}Th is of terrigenous origin, the stages 2 and 4 $^{230}Th_{ex}/^{232}Th$ minima and ^{232}Th maxima must reflect an increase of detrital sediment flux during glacial times. The $\delta^{18}O$ stratigraphy-derived sedimentation rates of non-$CaCO_3$ (terrigenous) material support this interpretation (Fig. 3), so do data on other drift sediment cores of the N. Atlantic [35,36].

3.4. Boundary scavenging at BOR: a comparison of ^{10}Be, ^{26}Al, and ^{230}Th

Preferential scavenging of ^{10}Be over ^{26}Al at BOR over the last 100 kyr has led to a much higher $(^{10}Be/^{26}Al)_a$, i.e. $^{10}Be/^{26}Al$ of atmospheric origin, in CH88-11P (Fig. 5a) than the atmospheric production ratio of 260 ± 40 [21]. The inverse relationship between $(^{10}Be/^{26}Al)_a$ and detrital flux (Fig. 5a vs. Fig. 3) rules out high terrigenous flux as being responsible for the enhanced ^{10}Be scavenging. The low glacial $(^{10}Be/^{26}Al)_a$ (Fig. 5a) may reflect a reduction in bioproductivity and/or water exchange between BOR and the open Atlantic. We will evaluate later these two possibilities using a mass-balance model.

At BOR, preferential scavenging of ^{10}Be over ^{230}Th also occurs during the Holocene (Fig. 5b), but the situation was reversed during the LGM. Given production rates of ~ 8.7 dpm/cm^2/kyr for ^{230}Th and 1.2×10^6 atoms/cm^2/yr [22] for ^{10}Be,

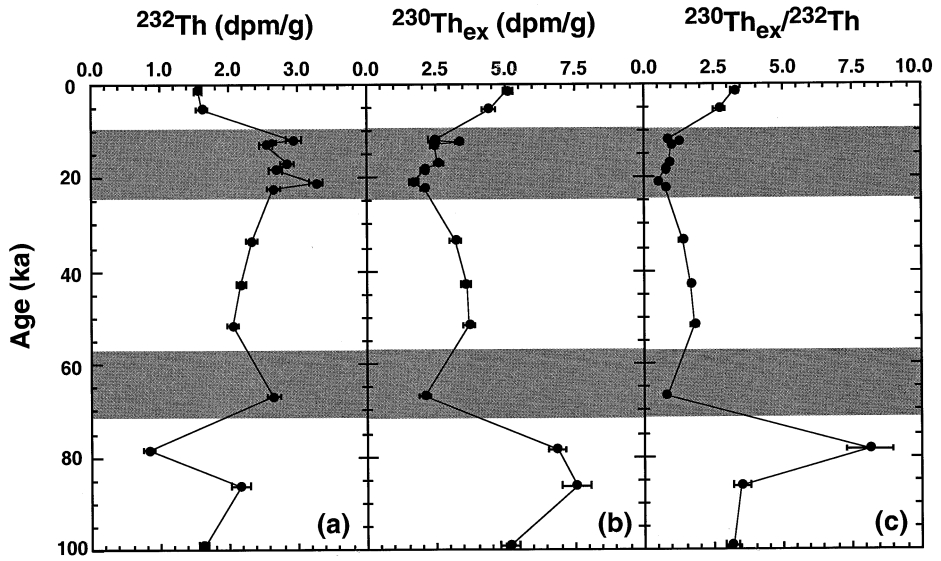

Fig. 4. (a) ^{232}Th, (b) ^{230}Th$_{ex}$, and (c) ^{230}Th$_{ex}$/^{232}Th in CH88-11P. The low ratios of ^{230}Th$_{ex}$/^{232}Th during glacial times reflect increased terrestrial sediment inputs to the area. Shaded areas delineate marine isotope stages 2 and 4.

CH88-11P should have a ^{10}Be/^{230}Th$_{ex}$ ratio of 1.4×10^{8} atoms/dpm barring lateral transport of ^{10}Be or ^{230}Th. This production ratio is exceeded by the Holocene ratios but is three times the LGM ratios in the core (Fig. 5b). The low LGM ratios cannot be attributed to changes in atmospheric production of ^{10}Be [29,37]. They most likely resulted from a preferential scavenging of ^{230}Th over ^{10}Be associated with the high terrigenous aluminosilicate (clay) flux during the LGM (Fig. 3).

That ^{26}Al/^{230}Th$_{ex}$ ratios are all lower than the production ratio of 5.4×10^{5} atoms/dpm at the core site (Fig. 5c) also indicates the efficient boundary scavenging of ^{230}Th. Owing to the strong affinity of Th to clay minerals [38], the high lithogenic flux into this N. Atlantic margin appears to preferentially scavenge ^{230}Th over ^{26}Al. An alternative explanation for the low ^{26}Al/^{230}Th$_{ex}$ and ^{10}Be/^{230}Th$_{ex}$ ratios would be a preferential transport of ^{26}Al and ^{10}Be relative to ^{230}Th via WBUC to the Southern Ocean. While this scenario would explain the high ^{10}Be/^{230}Th$_{ex}$ ratios in Antarctic sediments [32], it would require more ^{26}Al to be exported from BOR than ^{10}Be to satisfy the observed ^{10}Be/^{26}Al and ^{26}Al/^{230}Th$_{ex}$ ratios in CH88-11P (Fig. 5a). This seems unlikely in view of the short residence times of ^{26}Al and ^{230}Th compared to those of ^{10}Be in the ocean [1,2].

To conclude, the relative intensity in the boundary scavenging of ^{10}Be, ^{26}Al and ^{230}Th at BOR follows the orders $^{10}\mathrm{Be}\geq{}^{230}\mathrm{Th}>{}^{26}\mathrm{Al}$ during the Holocene and $^{230}\mathrm{Th}>{}^{10}\mathrm{Be}>{}^{26}\mathrm{Al}$ during the LGM. These sequences are at variance with the order $^{10}\mathrm{Be}>{}^{26}\mathrm{Al}\approx{}^{230}\mathrm{Th}$ expected from the relative particle reactivities for the three species [1,2,26]. The difference could stem from the much increased terrigenous influx of clays at BOR, which favor the scavenging of ^{230}Th. Apparently, ^{26}Al is much less sensitive to this boundary scavenging than either ^{230}Th or ^{10}Be, and as such, ratio ^{10}Be/^{26}Al as a proxy for paleoproductivity [1,2] stands on a firmer ground than ratio ^{10}Be/^{230}Th$_{ex}$. As shown in Section 3.6, along with authigenic ^{10}Be/^{9}Be and ^{26}Al/^{27}Al, ^{10}Be/^{26}Al can be used to quantitatively assess past changes in productivity and circulation of the study area.

3.5. *Boundary scavenging of ^{230}Th: cause and consequence*

The deposition of ^{230}Th$_{ex}$ in CH88-11P, about 17 dpm/cm^2/kyr in the Holocene and 56 dpm/cm^2/

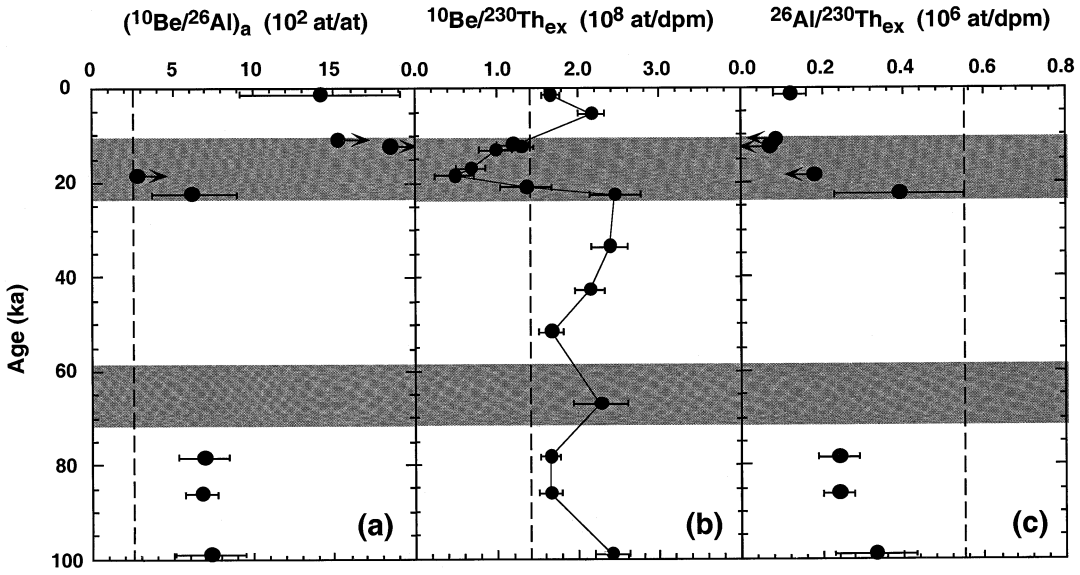

Fig. 5. (a) $(^{10}Be/^{26}Al)_a$, (b) $^{10}Be/^{230}Th_{ex}$, and (c) $^{26}Al/^{230}Th_{ex}$ in CH88-11P. ^{10}Be was corrected for the detrital contribution via Eq. 1. Vertical dashed lines represent the expected ratios if no differential deposition of the nuclides of interest takes place. These ratios are: (a) $^{10}Be/^{26}Al = 2.6 \times 10^2$ atom/atom, (b) $^{10}Be/^{230}Th = 1.4 \times 10^8$ atoms/dpm, and (c) $^{26}Al/^{230}Th = 0.53 \times 10^6$ atoms/dpm. The arrows in (a) indicate the lower limits of $^{10}Be/^{26}Al$, and in (c), the upper limits of $^{26}Al/^{230}Th_{ex}$. Shaded areas delineate marine isotope stages 2 and 4.

kyr during the LGM, is higher than the water-column production by a factor of 2 and 6.4, respectively. Sediment-trap data from a middle Atlantic bight (MAB) site (water depth 2752 m) to the north show $^{230}Th_{ex}$ flux-to-production ratios of 1.9, 2.0, and 2.2 at 452 m, 1757 m, and 2702 m, respectively [27]. The similarity of these ratios and their agreement with the Holocene ratio in CH88-11P indicate that (a) the collection efficiencies of these sediment traps are reasonably stable, (b) contributions of resuspended sediments from the sea floor to each of these traps are minimal, and (c) an intensified boundary scavenging of ^{230}Th results in its higher than production flux. This last indication has not been fully appreciated, since unlike radiotracers such as ^{231}Pa and ^{10}Be, ^{230}Th has a very short oceanic residence time and its horizontal transport has generally been considered quite limited. Nevertheless, recent studies have increasingly pointed to the lateral migration of ^{230}Th. Evidence comes from measurements and modeling of ^{230}Th in seawater [39–41] as well as in particulates collected by sediment traps and cores ([27,43,44], this work). For example, the flux-to-production ratio of ^{230}Th at MAB increases considerably toward the coast, reaching values of >10 at water depths <500 m [27]. Over 90% of the ^{230}Th in this ocean-margin area could thus originate from the open Atlantic. As has been noted at MAB [27], the well-defined linear correlations between $^{230}Th_{ex}$ in sediment-trap/core material and water depth, and the lack of similar increases in the fluxes of ^{210}Pb and ^{231}Pa argue against sediment focusing as a mechanism for the high local $^{230}Th_{ex}$ inventories. The low $^{26}Al/^{230}Th_{ex}$ ratio in CH88-11P (Fig. 5c) also speaks against sediment focusing. As the production ratio of $^{26}Al/^{230}Th_{ex}$ increases with decreasing water depth, focusing of sediments locally or from shallow depths should not lower $^{26}Al/^{230}Th_{ex}$. A comparison of $^{10}Be/^{230}Th_{ex}$ between the BOR and MAB sediments further suggests that sediment focusing cannot be the cause for the high $^{230}Th_{ex}$ flux-to-production ratios at BOR. Were it the cause, one would expect similar $^{10}Be/^{230}Th_{ex}$ ratios in both BOR and MAB sediments, considering that a major source of the BOR sediments comes from the continental slope at MAB

via WBUC [9]. However, $^{10}Be/^{230}Th_{ex}$ in MAB sediments at ~400–3000 m water depths centers around $(9 \pm 2) \times 10^8$ atoms/dpm [27] which is ~5 times the Holocene ratio and 20 times the LGM ratio in BOR sediments (Fig. 5b). Sediments on their transit from MAB via WBUC must have their sorbed isotopes re-equilibrated with those in the water. In this way, depositional fluxes of ^{10}Be and ^{230}Th depend on their concentrations and residence times in BOR deep water. The low BOR $^{10}Be/^{230}Th_{ex}$ ratios chiefly reflect increased $^{230}Th_{ex}$ fluxes resulting from the short residence time [23] and increased concentration [41] of ^{230}Th in BOR deep water.

What causes the preferential scavenging of ^{230}Th over ^{10}Be, and what drives the boundary scavenging of ^{230}Th in general? As has been discussed in the case of preferential scavenging of ^{230}Th over ^{231}Pa [38], we believe that clay particles play an important role.

Table 2 shows that $^{10}Be/^{230}Th$ is much higher in deep water than in seafloor sediments at three locations. In the clay-rich BOR and the carbonate-rich equatorial Pacific, $F_{Th/Be} \approx 10$ – a manifestation to preferential scavenging of ^{230}Th and to the fact that clays, not carbonates, are the major carrier for both ^{10}Be and ^{230}Th [38,46,47]. The Antarctic opal-rich sediments show $F_{Th/Be} \approx 2$, apparently resulting from a smaller ^{230}Th–^{10}Be fractionation by opaline particles. The large difference in $F_{Th/Be}$ between the equatorial Pacific and the Antarctic implies that the higher $^{10}Be/^{230}Th_{ex}$ ratios in Antarctic sediments (Table 2) may not necessarily reflect a higher productivity in the Antarctic than in the equatorial Pacific; it reflects rather the low-clay, high-opal lithology of Antarctic sediments. By the same token, that ^{230}Th scavenging in the Weddell Sea (where the terrigenous flux is low) can be as low as one third of its water-column production [43], in sharp contrast to that at BOR, points further to the association of ^{230}Th scavenging with the flux of clays.

It could be argued that a weakened ocean circulation during the LGM might have decreased the scavenging of ^{230}Th at BOR. But this decrease would have been overridden by the effect of an increased terrigenous clay flux. In contrast to a ten-fold Holocene-to-LGM increase in clay flux (Fig. 3), the $^{230}Th_{ex}$ flux at BOR increased by ~3 times from ~17 dpm/cm^2/kyr to ~56 dpm/cm^2/kyr. If the distribution coefficient (K_d) of ^{230}Th between clays and seawater remained unchanged at the site, the combined effect of a decreased water mixing rate and an increased clay flux would have reduced the deep-water ^{230}Th concentrations at BOR by a factor of ≥ 3. Without the weakening of ocean circulation, the increased clay flux might have caused even greater boundary scavenging of ^{230}Th at BOR.

The above analysis provides a cautionary note on the use of $^{10}Be/^{230}Th_{ex}$ as a proxy for paleoparticle flux [32]. It also echoes recent concerns [43,44] in regard to possible over- or underestimation of particle rain rates by the ^{230}Th-normalized method.

3.6. Past changes in ocean productivity and water circulation at BOR

A two-box model, consisting of a BOR box (area $A_B = \sim 700 \times 700$ km^2 and water depth $z_B = 3000$ m [9]) and an open-ocean box, is set

Table 2
Estimates of fractionation factors[a] between ^{230}Th and ^{10}Be ($F_{Th/Be}$) for different sediment types

Location	Sediment type	$(^{10}Be/^{230}Th)^b_w$	$(^{10}Be/^{230}Th_{ex})^b_s$	$F_{Th/Be}$
BOR	clay	17 ± 3 ($n = 17$)	1.7 ± 0.1 ($n = 1$)	10 ± 2
S. Atlantic (>50°S)	opaline ooze	12 ± 3 ($n = 12$)	6 ± 2 ($n = 4$)	2.0 ± 0.8
Eq. Pacific	calcareous ooze	12 ± 2 ($n = 22$)	1.1 ± 0.3 ($n = 12$)	11 ± 3

[a] $F_{Th/Be} = (^{10}Be/^{230}Th)_w/(^{10}Be/^{230}Th_{ex})_s$ where subscripts w and s denote water (>3000 m) and surface sediments, respectively. $F_{Th/Be} > 1$ indicates preferential scavenging of ^{230}Th over ^{10}Be by sediment particles.
[b] The ratios (in 10^8 atoms/dpm) were based on data reported in [16,45] for ^{10}Be and [40–42] for ^{230}Th in deep water, and ([14,31,32], this work) for $^{10}Be/^{230}Th_{ex}$ in sediments. Shown in parentheses is the number (n) of measurements. $F_{Th/Be}$ for other high-particle flux ocean margins were not estimated because of the very limited data base on $^{10}Be/^{230}Th_{ex}$ in deep waters.

up for the mass balance of dissolved Be and Al isotopes at BOR. The model assumes water entering BOR from the North Atlantic; it does not specify where the water leaves though it may exit mainly to the south via WBUC. Let k_w (yr^{-1}) be the BOR water replacement rate constant, mass balance of authigenic ^{10}Be and ^{9}Be in the BOR box requires:

$$P_{Be10}/z_B + C^O_{Be10}\times k_w = C^B_{Be10}\times k_{Be} + C^B_{Be10}\times k_w \quad (4)$$

and

$$f_{Be9}\times a_{Be}\times F_p/z_B + C^O_{Be9}\times k_w = C^B_{Be9}\times k_{Be} + C^B_{Be9}\times k_w \quad (5)$$

where P_{Be10} is ^{10}Be production rate (atoms/cm^2/yr), F_p is deposition rate (g/cm^2/yr) of terrigenous particles with ^{9}Be concentration a_{Be} (atoms/g), of which a fraction f_{Be9} is soluble, k_{Be} is scavenging rate constant (yr^{-1}) of Be, and C is concentration (atoms/cm^3) in seawater (superscripts O and B denoting the open-ocean and BOR boxes, respectively).

Assuming the deposition rate of ^{26}Al to equal its production rate, P_{Al26}, we estimate the deposition rate of ^{10}Be (F_{Be10}) from $(^{10}Be/^{26}Al)_a$ in BOR sediments:

$$F_{Be10} = C^B_{Be10}\times k_{Be}\times z_B = P_{Al26}\times\left(\frac{^{10}Be}{^{26}Al}\right)_a \quad (6)$$

From Eqs. 4–6, k_w and F_p are solved as:

$$k_w = \frac{\left[\left(\frac{^{10}Be}{^{26}Al}\right)_a\times P_{Al26} - P_{Be10}\right]}{(C^O_{Be10} - C^B_{Be10})\times z_B} \quad (7)$$

and

$$F_p = \left[\frac{(P_{Be10} + k_w C^O_{Be10} z_B)}{\left(\frac{^{10}Be}{^{9}Be}\right)_a} - k_w C^O_{Be9} z_B\right]\left(\frac{1}{f_{Be9} a_{Be}}\right) \quad (8)$$

In Eqs. 6–8, subscript a denotes authigenic. Measurable quantities include $(^{10}Be/^{26}Al)_a$, $(^{10}Be/^{9}Be)_a$, and f_{Be9}. Assignable quantities include $P_{Be10} = 1.2\times10^6$ atoms/cm^2/yr [22], $P_{Al26}/P_{Be10} = 3.8\times10^{-3}$ [21], and $a_{Be} = 2.8$ ppm [18]. C^B_{Be10} can be estimated from $(^{10}Be/^{9}Be)_a$ by assuming $C^B_{Be9} = 25\pm5$ pM [16]. We assume $C^O_{Be10} = 800\pm100$ atoms/g and $C^O_{Be9} = 25\pm5$ pM based on modern ocean measurements [16].

Table 1 lists the modeled k_w and F_p, with uncertainties estimated from the analytical errors of ^{26}Al and ^{10}Be. A $\pm20\%$ uncertainty of ^{10}Be production rate [22] would raise the quoted errors by 10–40%. Results show a Holocene water replacement time ($=1/k_w$) of about 23 yr at BOR. While in line with a generally sluggish deep-water circulation in the North Atlantic during the last glaciation [48], our results show quantitatively that the deep-water circulation at BOR was about 5 times slower during the LGM than during the Holocene.

The modeled terrestrial flux (F_p) to BOR increases from 3.7 mg/cm^2/yr in the Holocene to >29 mg/cm^2/yr in the LGM (Table 1), consistent with the observed flux (Fig. 3). To retrieve information on past changes in ocean productivity, we first link the total particle (lithogenic+biogenic) flux (F_p*) to the water-column residence time of ^{10}Be (τ_{Be}) via the following relationship and then evaluate the productivity from (F_p*$-F_p$):

$$F^*_p = \frac{F_{Be10}}{C_{Be10,p}} = \frac{z_B}{K_{d,Be10}\tau_{Be}} \quad (9)$$

where F_p* is the flux (g/cm^2/yr) of all sinking particles having an overall ^{10}Be concentration (atoms/g) of $C_{Be10,p}$, and $K_{d,Be10}$ ($=C_{Be10,p}/C_{Be10}$) is distribution coefficient (cm^3/g) of ^{10}Be between particles and seawater. $K_{d,Be10}$ (see Fig. 6) increases from $\sim2\times10^5$ in surface waters to $\sim5\times10^5$ in deep waters, due probably to the remineralization of biogenic particles. At BOR, $K_{d,Be10}$ has a value of $\sim4\times10^5$. Re-arranging Eq. 6,

$$\tau_{Be} = \frac{1}{k_{Be}} = \frac{C^B_{Be10}\times z_B}{P_{Al26}\times\left(\frac{^{10}Be}{^{26}Al}\right)_a} \quad (10)$$

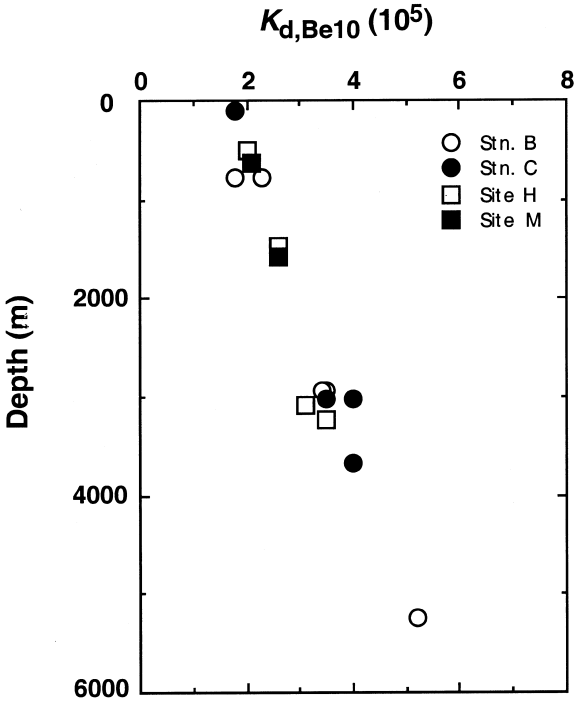

Fig. 6. Variation of distribution coefficients of ^{10}Be ($K_{d,Be10}$) with water depth. $K_{d,Be10}$ is estimated from data on sediment-trap material (averaged over different seasons to remove the seasonal influence on particulate compositions) and ambient seawater. Data source: [45,46], and our unpublished results.

we calculated τ_{Be} and F_p* from Eqs. 9 and 10 for different time periods and showed (Table 1) that τ_{Be} has a range of 5–35 yr, which is very close to that of ^{26}Al, an order smaller than that in the open Atlantic [16].

Table 1 shows that the total particle flux (F_p*) varies from 20–138 mg/cm^2/yr, of which lithogenic flux (F_p) constitutes $\sim$10% during the Holocene but $\sim$30% during the LGM. The increase of lithogenic flux is consistent with the high LGM continental input discussed earlier. Our model results are further validated by the agreement between the modeled Holocene flux of 40 ± 14 mg/cm^2/yr (Table 1) and the sediment-trap measurements of 66 ± 33 mg/cm^2/yr and 20 ± 15 mg/cm^2/yr respectively from water depth of 2397 m and 3170 m at an adjacent station (35°N, 74°W) [27]. Our F_p* for the LGM could be an upper-limit estimate, as the clay-rich LGM sediments may lead to a higher $K_{d,Be10}$ [46].

The net biogenic particle flux (or export productivity, F_p*$-F_p$) has remained little changed except during the deglaciation when a much higher productivity occurred (Table 1). This is supported by the carbonate flux signals in CH88-11P (Fig. 3), although the signals are uncorrected for dissolution. Deglaciation caused the sea to rise about 130 m in a relatively short period [49] and it could have flooded much of the continental shelf. It could also have enhanced river runoff and local vertical mixing. Fresh water input may further induce buoyancy-forced onshore movement of deep water thus enhancing upwelling at ocean margins [50]. Whether these and other factors might have spurred the regional productivity remains speculative.

4. Summary

This study explores several important applications of ^{26}Al, ^{10}Be and U–Th isotopes on past changes in continental input, ocean productivity and water mixing in an ocean margin. ^{26}Al was measured for the first time in such a depositional setting of high ^{27}Al flux. Results show a marked decrease in both ^{26}Al/^{27}Al and ^{10}Be/^{9}Be in BOR deep water during LGM, reflecting a greatly enhanced delivery of terrigenous material to the site. This enhancement caused changes in the relative intensity of radionuclide scavenging at BOR. The boundary scavenging during the Holocene follows the order ^{10}Be $\geq$ ^{230}Th $>$ ^{26}Al whereas during LGM, the order became ^{230}Th $>$ ^{10}Be $>$ ^{26}Al. Both sequences, however, are at variance with the order ^{10}Be $>$ ^{26}Al $\approx$ ^{230}Th as anticipated from the relative particle reactivities of the three species. Arguments are presented to show that dissolved ^{230}Th and ^{10}Be are subject to considerable lateral transport in areas of high particle input such as ocean margins, that changes in clay influx to such areas may affect the scavenging of ^{230}Th, and that ratio ^{10}Be/^{26}Al is a more promising proxy than ratio ^{10}Be/^{26}Al for paleoceanographic reconstructions.

At BOR, ocean productivity have remained little changed over the last 100 kyr except during the last deglaciation when it significantly increased.

Furthermore, the water replacement rate increased five-fold from LGM to the Holocene.

Acknowledgements

We thank T.C. Johnson of Duke University for letting us sample core CH88-11P. Comments made by EPSL reviewers and editor greatly helped improve our presentation. This work was supported by the NSF Chemical Oceanography Program under grant OCE-9633469.*[EB]*

References

[1] T.L. Ku, L. Wang, S. Luo, J.R. Southon, ^{26}Al in sea water and ^{26}Al/^{10}Be as paleo-flux tracer, Geophys. Res. Lett. 22 (1995) 2163–2166.

[2] L. Wang, T.L. Ku, S. Luo, J.R. Southon, M. Kusakabe, ^{26}Al-^{10}Be systematics in deep-sea sediments, Geochim. Cosmochim. Acta 60 (1996) 109–119.

[3] D. Lal, B. Peters, Cosmic-ray produced radioactivity on the Earth, in: Handbuch der Physik 46/2, Springer, Berlin, 1967, pp. 551–612.

[4] J.L. Reyss, Y. Yokoyama, F. Guichard, Production cross sections of ^{26}Al, ^{22}Na, ^{7}Be from argon and of ^{7}Be, ^{10}Be from nitrogen: Implications for production rates of ^{26}Al and ^{10}Be in the atmosphere, Earth Planet. Sci. Lett. 53 (1981) 203–210.

[5] R. Middleton, J. Klein, ^{26}Al: measurement and applications, Philos. Trans. R. Soc. Lond. A 323 (1987) 121–143.

[6] D. Bourles, G.M. Raisbeck, F. Yiou, M. Loiseaux, M. Lieuvin, J. Klein, R. Middleton, Investigation of the possible association of ^{10}Be and ^{26}Al with biogenic matter in the marine environments, Nucl. Instrum. Methods Phys. Res. B 5 (1984) 365–370.

[7] P. Sharma, J. Klein, R. Middleton, T.M. Church, ^{26}Al and ^{10}Be in authigenic marine minerals, Nucl. Instrum. Methods Phys. Res. B 29 (1987) 335–340.

[8] P. Sharma, T.M. Church, M. Bernat, Use of cosmogenic ^{10}Be and ^{26}Al in philistine for the dating of marine sediments in the south Pacific ocean, Chem. Geol. 73 (1989) 279–288.

[9] B.J. Haskell, T.C. Johnson, W.J. Showers, Fluctuations in deep western north Atlantic circulation on the Blake Outer Ridge during the last deglaciation, Paleoceanography 6 (1991) 21–31.

[10] M. Schwartz, S.P. Lund, T.C. Johnson, Environmental factors as complicating influences in the recovery of the quantitative geomagnetic-field paleointensity estimates from sediments, Geophys. Res. Lett. 23 (1996) 2693–2996.

[11] L.D. Keigwin, G.A. Jones, Glacial-Holocene stratigraphy, chronology, and paleoceanographic observations on some North Atlantic sediment drifts, Deep-Sea Res. 36 (1989) 845–867.

[12] L.D. Keigwin, G.A. Jones, Western North Atlantic evidence for millennial-scale changes in ocean circulation and climate, J. Geophys. Res. 99 (1994) 12397–12410.

[13] J.R. Southon, J.S. Vogel, I. Nowikow, D.E. Nelson, R.G. Korteling, T.L. Ku, M. Kusakabe, C.A. Huh, The measurement of ^{10}Be concentrations with a tandem accelerator, Nucl. Instrum. Methods Phys. Res. 205 (1982) 251–257.

[14] L. Wang, ^{26}Al-^{10}Be Systematics in the Ocean, Ph.D. Thesis, University of Southern California, Los Angeles, CA, 1997, 261 pp.

[15] D. Bourles, G.M. Raisbeck, F. Yiou, ^{10}Be and ^{9}Be in marine sediments and their potential for dating, Geochim. Cosmochim. Acta 53 (1989) 443–452.

[16] T.L. Ku, M. Kusakabe, C.I. Measures, J.R. Southon, G.L. Cusimano, J.S. Vogel, D.E. Nelson, S. Nakaya, Beryllium isotope distribution in the western North Atlantic: a comparison to the Pacific, Deep-Sea Res. 37 (1990) 795–808.

[17] L. Brown, I.S. Sacks, F. Tera, J. Klein, R. Middleton, Beryllium-10 in continental sediments, Earth Planet. Sci. Lett. 55 (1981) 370–376.

[18] S.R. Taylor, Abundance of chemical elements in the continental crust: a new table, Geochim. Cosmochim. Acta 28 (1964) 1273–1286.

[19] C.I. Measures, J.M. Edmond, T.D. Jickell, Aluminum in the northwest Atlantic, Geochim. Cosmochim. Acta 50 (1986) 1423–1429.

[20] K.J. Orians, K.W. Bruland, The biogeochemistry of aluminum in the Pacific Ocean, Earth Planet. Sci. Lett. 78 (1986) 397–410.

[21] G.M. Raisbeck, F. Yiou, J. Klein, R. Middleton, Accelerator mass spectrometry measurement of cosmogenic ^{26}Al in terrestrial and extraterrestrial matter, Nature 301 (1983) 690–692.

[22] M.C. Monaghan, S. Krishnaswami, K.K. Turekian, The global-average production rate of ^{10}Be, Earth Planet. Sci. Lett. 76 (1985/86) 279–287.

[23] E. Yu, Variations in the Particulate Flux of ^{230}Th and ^{231}Pa and Paleoceanographic Applications of the ^{231}Pa/^{230}Th ratio, Ph.D. Thesis, Woods Hole Oceanographic Institution/Massachusetts Institute of Technology, 1994, 269 pp.

[24] T.H. Peng, T.L. Ku, J. Southon, C. Measures, W.S. Broecker, Factors controlling the distribution of ^{10}Be and ^{9}Be in the ocean, in: K. Gopalan (Ed.), From Mantle to Meteorites, Acad. Sci., Bangalore, 1990, pp. 201–204.

[25] R.W. Murray, M. Leinen, Scavenged excess aluminum and its relationship to bulk titanium in biogenic sediment from the central equatorial Pacific Ocean, Geochim. Cosmochim. Acta 60 (1996) 3869–3878.

[26] R.F. Anderson, Y. Lao, W.S. Broecker, S.E. Trumbore, H.J. Hofmann, W. Wolfli, Boundary scavenging in the Pacific Ocean: a comparison of ^{10}Be and ^{231}Pa, Earth Planet. Sci. Lett. 96 (1990) 287–304.

[27] R.F. Anderson, M.Q. Fleisher, P.E. Biscaye, N. Kumar, B. Dittrich, P. Kubik, M. Suter, Anomalous boundary scavenging in the Middle Atlantic Bight: evidence from ^{230}Th, ^{231}Pa, ^{10}Be and ^{210}Pb, Deep-Sea Res. 41 (1994) 537–561.

[28] Y. Lao, R.F. Anderson, W.S. Broecker, S.E. Trumbore, H.J. Hofmann, W. Wolfli, Transport and burial rates of ^{10}Be and ^{231}Pa in the Pacific Ocean during the Holocene period, Earth Planet. Sci. Lett. 113 (1992) 173–189.

[29] Y. Lao, R.F. Anderson, W.S. Broecker, S.E. Trumbore, H.J. Hofmann, W. Wolfli, Increased production of cosmogenic ^{10}Be during the last glacial maximum, Nature 357 (1992) 576–578.

[30] M. Frank, J. Eckhardt, A. Eisenhauer, P.W. Kubik, B. Dittrich-Hannen, M. Segl, A. Mangini, Beryllium 10, thorium 230, and protactinium 231 in Galapagos microplate sediments: Implications of hydrothermal activity and paleoproductivity changes during the last 100,000 years, Paleoceanography 9 (1994) 559–578.

[31] M. Frank, A. Eisenhauer, W.J. Bonn, P. Walter, H. Grobe, P.W. Kubik, B. Dittrich-Hannen, A. Mangini, Sediment distribution versus paleoproductivity change: Weddell Sea margin sediment stratigraphy for the last 250,000 years deduced from ^{230}Th$_{ex}$, ^{10}Be and biogenic barium profiles, Earth Planet. Sci. Lett. 136 (1995) 559–573.

[32] N. Kumar, R.F. Anderson, R.A. Mortlock, P.N. Froelich, P. Kubik, B. Dittrich-Hannen, M. Suter, Increased biological productivity and export production in the glacial Southern Ocean, Nature 378 (1996) 675–680.

[33] K.K. Turekian, K.H. Wedepohl, Distribution of the elements in some major units of the Earth's crust, Geol. Soc. Am. Bull. 72 (1961) 175–192.

[34] T.L. Ku, Uranium Series Disequilibrium in Deep-Sea Sediments, Ph.D. Thesis, Columbia University, New York, 1966.

[35] M.P. Bacon, J.N. Rosholt, Accumulation rates of Th-230, Pa-231, and some transition metals on the Bermuda Rise, Geochim. Cosmochim. Acta 46 (1982) 651–666.

[36] R. Francois, M.P. Bacon, Variations in terrigenous input into the deep Equatorial Atlantic during the past 24,000 years, Science 251 (1991) 1473–1476.

[37] M. Frank, B. Schwarz, S. Baumann, P.W. Kubik, M. Suter, A. Mangini, A 200 kyr record of cosmogenic radionuclide production rate and geomagnetic field intensity from ^{10}Be in globally-stacked deep-sea sediments, Earth Planet. Sci. Lett. 149 (1997) 121–129.

[38] S. Luo, T.L. Ku, Oceanic ^{231}Pa/^{230}Th ratio influenced by particle composition and remineralization, Earth Planet. Sci. Lett. 167 (1999) 183–195.

[39] S. Vogler, J. Scholten, M. Rutgers van der Loeff, A. Mangini, ^{230}Th in the eastern North Atlantic: the importance of water mass ventilation in the balance of ^{230}Th, Earth Planet. Sci. Lett. 156 (1998) 61–74.

[40] M.M. Rutgers van der Loeff, G.W. Berger, Scavenging of ^{230}Th and ^{231}Pa near the Antarctic Polar Front in the South Atlantic, Deep-Sea Res. 40 (1993) 339–357.

[41] S.B. Moran, M.A. Charette, J.A. Hoff, R.L. Edwards, W.M. Landing, Distribution of ^{230}Th in the Labrador Sea and its relation to ventilation, Earth Planet. Sci. Lett. 150 (1997) 151–160.

[42] Y. Nozaki, T. Nakanishi, ^{231}Pa and ^{230}Th profiles in the open ocean water column, Deep-Sea Res. 32 (1985) 1209–1220.

[43] H.J. Walter, M.M. Rutger van der Loeff, H. Holtzen, U. Bathmann, Reduced scavenging of ^{230}Th in the Weddell Sea: implications for paleoceanographic reconstructions in the South Atlantic, Deep-Sea Res. 47 (2000) 1369–1387.

[44] G.M. Henderson, C. Heinze, R.F. Anderson, A.M.E. Winguth, Global distribution of the ^{230}Th flux to ocean sediments constrained by GCM modeling, Deep-Sea Res. 46 (1999) 1861–1893.

[45] M. Kusakabe, T.L. Ku, J.R. Southon, J.S. Vogel, D.E. Nelson, C.I. Measures, Y. Nozaki, Distribution of ^{10}Be and ^{9}Be in the Pacific Ocean, Earth Planet. Sci. Lett. 82 (1987) 231–240.

[46] P. Sharma, R. Mahannah, W.S. Moore, T.L. Ku, J.R. Southon, Transport of ^{10}Be and ^{9}Be in the ocean, Earth Planet. Sci. Lett. 86 (1987) 69–76.

[47] J.R. Southon, T.L. Ku, D.E. Nelson, J.L. Reyss, J.C. Duplessy, J.S. Vogel, ^{10}Be in a deep-sea core: Implications regarding ^{10}Be production changes over the past 420 ka, Earth Planet. Sci. Lett. 85 (1987) 356–364.

[48] E.A. Boyle, L.D. Keigwin, Deep circulation of the North Atlantic over the last 200,000 years: geochemical evidence, Science 218 (1982) 784–787.

[49] R.G. Fairbanks, 17,000-year glacio-eustatic sea level record: influence of glacial melting rates on the Younger Dryas event and deep-ocean circulation, Nature 342 (1989) 637–742.

[50] C.T.A. Chen, The Three Gorges Dam: Reducing the upwelling and thus productivity in the East China Sea, Geophys. Res. Lett. 27 (2000) 381–383.